

Massive-lepton-pair production in a modified quark-parton model

J. B. Choi, H. W. Lee, I. S. Ko, and H. S. Song

Department of Physics, College of Natural Science, Seoul National University, Seoul, Korea

Kwang Sup Soh

Hoikidong, Dongdemunku, Seoul, Korea

(Received 7 June 1977)

Lepton-pair production in the process $p + p \rightarrow l^+ + l^- + X$ is considered using a quark-gluon-parton model. Scaling behavior is studied and the results of calculations on $d^2\sigma/dm dy$ and $d\sigma/dm$ are compared with experiments at Brookhaven, Fermilab, and CERN ISR.

I. INTRODUCTION

Direct lepton-pair production (μ^\pm or e^\pm) in hadron-hadron collisions has received much interest both from theoreticians and experimentalists. The original Drell-Yan parton annihilation model¹ and subsequent similar works² used the quark-parton model (QPM)³ which has had some notable successes in the $e(\nu)N$ reactions in the deep-inelastic region and in the $e^+e^- \rightarrow$ hadrons processes.

A modified QPM⁴ was considered by one of us (K.S.) to compute the structure functions of the $e(\nu)N$ deep-inelastic inclusive processes. In the conventional QPM's the gluons which carry approximately half of a nucleon momenta do not contribute to the deep-inelastic-scattering cross sections. In the modified QPM the gluons play more important roles. A nucleon is composed of valence quarks and gluons only, and the "sea" of the $q-\bar{q}$ pairs of the conventional QPM's shows up owing to the quark pair production of the gluons. The gluons produce $q-\bar{q}$ pairs which interact with a virtual photon [massive vector bosons in the $\nu(\bar{\nu})$ scattering] of the deep-inelastic processes.

In this paper we use the modified QPM for a study of the process

$$p + p \rightarrow l^+ + l^- + X. \tag{1}$$

A gluon parton in one proton and a quark parton in the other produce a virtual photon via Compton-like scattering, and the photon subsequently decays into a lepton pair as shown in Fig. 1.

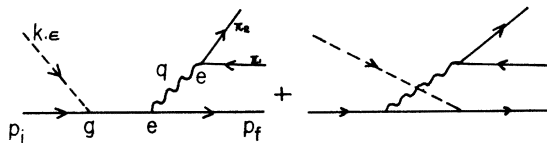


FIG. 1. Feynman diagram of Compton-like scattering. The dashed line represents the gluon; the wavy line represents the photon.

To compare with experimental data we take the same parton distribution functions as in Ref. 4, i.e.,

$$g(x) = 2 \frac{(1-x)^3}{x} \tag{2}$$

for the gluon parton⁵ and

$$u(x) = 0.594 \frac{(1-x^2)^3}{\sqrt{x}} + 0.461 \frac{(1-x^2)^5}{\sqrt{x}} + 0.621 \frac{(1-x^2)^7}{\sqrt{x}}, \tag{3a}$$

$$d(x) = 0.072 \frac{(1-x^2)^3}{\sqrt{x}} + 0.206 \frac{(1-x^2)^5}{\sqrt{x}} + 0.621 \frac{(1-x^2)^7}{\sqrt{x}} \tag{3b}$$

for the up and the down quarks, respectively. Here x denotes the fractional longitudinal momentum of a parton. The quark distribution functions are from Barger *et al.*,^{6,7} and the coupling constant g_s of gluon-quark interaction is taken to be

$$\alpha_s \equiv \frac{g_s^2}{4\pi} = 0.32, \tag{4}$$

as in Ref. 4. This value is consistent with other works.⁸

Using these parameters of the deep-inelastic case, we will show in Sec. III that our computation agrees very well with recent high-energy experimental data.⁹⁻¹² In our calculation we take into account the color degrees of freedom.

In Sec. II we present the detailed calculations of the cross section $d^2\sigma/dq^2 dy$, and the result is compared with experimental data in Sec. III. A summary is given in Sec. IV.

II. CALCULATIONS

Consider the lepton-pair production in the proton-proton scattering as in Eq. (1). In our model the lepton pair is created by a virtual photon which

is produced by the Compton-like scattering of a gluon in one proton and a quark in the other. The amplitude of the gluon-quark scattering, shown in Fig. 1, is

$$\mathfrak{M} = \frac{e^2 g_s}{q^2} \left[\bar{u}(p_f) \gamma_\nu \frac{1}{\not{p}_i + \not{k} - M} \not{\epsilon} u(p_i) \bar{u}(\pi_2) \gamma^\nu v(\pi_1) + \bar{u}(p_f) \not{\epsilon} \frac{1}{\not{p}_i - \not{q} - M} \gamma_\nu u(p_i) \bar{u}(\pi_2) \gamma^\nu v(\pi_1) \right], \quad (5)$$

where p_i and p_f are the initial and the final quark momenta, respectively; π_1 and π_2 are the momenta of lepton pairs; and q is the momentum of the photon. The momentum and the polarization of the gluon are denoted by k and ϵ , respectively, and M is the quark mass. The $SU(3)_{\text{color}}$ λ matrices are omitted for simplicity, and the overall numerical factor due to color is given later.

After performing necessary trace evaluation and phase integration we obtain

$$\frac{d\sigma}{d^4q} = \frac{\alpha^2 \alpha_s}{18\pi} \frac{1}{q^2} \frac{(q^2 - k \cdot q)^2 + (2k \cdot p_i - k \cdot q)^2}{(k \cdot p_i)^2 (k \cdot p_f)} \times \delta^+(q^2 + 2k \cdot p_i - 2k \cdot q - 2p_i \cdot q), \quad (6)$$

and

$$\frac{d^2\sigma}{dq^2 dy} = \frac{\alpha^2 \alpha_s}{36} \frac{1}{q^4} \frac{\tau}{y_1 + y_2} \left\{ y_2 \int \int dx_1 dx_2 \frac{[(2y_1/x_1 - 1)^2 + (2x_2/y_2 - 1)^2] D(x_1, x_2)}{x_1 x_2^2 (x_2/y_2) (x_2/y_2 - 1)} + (x_1 \leftrightarrow x_2, y_1 \leftrightarrow y_2) \right\}. \quad (11)$$

Here $D(x_1, x_2) = g(x_1) [\frac{4}{9}u(x_2) + \frac{1}{9}d(x_2)]$. The second term inside the curly brackets is obtained by the substitution $x_1 \leftrightarrow x_2$ and $y_1 \leftrightarrow y_2$, which says that the parent protons of the gluon and the quark are interchanged. The numerical values of x_1 and x_2 are obviously limited as $0 < x_1, x_2 < 1$. The integration ranges of Eq. (11) are further limited by the δ^+ function in Eq. (6), and we find for the first integrand

$$y_1 \left(1 + \frac{\epsilon}{x_2/y_2 - 1} \right) < x_1 < 1, \quad (12)$$

$$y_2 \left(1 + \frac{\epsilon}{x_1/y_1 - 1} \right) < x_2 < 1,$$

with $\epsilon = M^2/q^2$. For the second integrand we make the substitution $x_1 \leftrightarrow x_2$, $y_1 \leftrightarrow y_2$.

It is well known that the Drell-Yan picture^{1,2} exhibits scaling behavior while the present model has logarithmic violation of scaling. To see how large this explicit breaking of scaling behavior is, we rewrite the cross section as

$$\frac{d^2\sigma}{dq^2 dy} = \frac{4\pi \alpha^2}{3q^4} F(\tau, y, s). \quad (13)$$

$$\frac{d^2\sigma}{dq^2 d(q \cdot k)} = \frac{\alpha^2 \alpha_s}{36} \frac{1}{q^2} \frac{(q^2 - k \cdot q)^2 + (2k \cdot p_i - k \cdot q)^2}{(k \cdot p_i)^3 (k \cdot p_f)}, \quad (7)$$

where we neglected quark mass compared with $k \cdot p_i$, $k \cdot p_f$, and q^2 .

At this stage it is convenient to introduce the scaling variables

$$\tau = \frac{q^2}{s}, \quad y = \frac{2Q_L}{\sqrt{s}}, \quad (8)$$

with Q_L denoting the longitudinal momentum of the lepton pair in the proton-proton c.m. system, and s the c.m. energy squared of the two protons. Another set of variables y_1 and y_2 is defined as

$$y_1 = \frac{y + (y^2 + 4\tau)^{1/2}}{2}, \quad y_2 = \frac{-y + (y^2 + 4\tau)^{1/2}}{2}. \quad (9)$$

Now, summation over all the gluon and quark momentum distributions is in order. Denoting x_1 and x_2 as the fractional momentum of partons, i.e.,

$$k = x_1 P, \quad p_i = x_2 \bar{P}, \quad (10)$$

where P is the momentum of one proton and \bar{P} is that of the other, we get the differential cross section

Since F is a function of τ and y in the Drell-Yan mechanism (scaling), the dependence on s represents how much the scaling is broken. In Fig. 2 we plot F versus s for given τ and y . There is only negligible s dependence for a large value of s . We have checked for different τ and y values, and the tendency of Fig. 2 still holds in these cases.

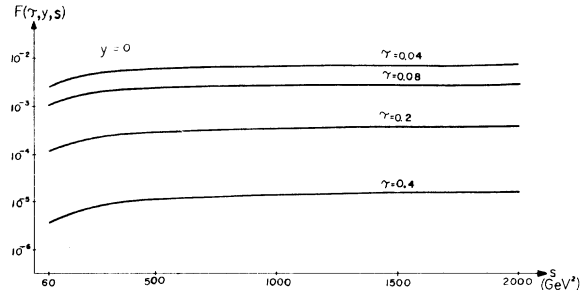


FIG. 2. Scaling behavior of $F(\tau, y, s)$. We plot F versus s for given τ and $y=0$. We see that for about $s < 300 \text{ GeV}^2$ the scaling is not well established in our model.

III. COMPARISON WITH EXPERIMENTAL DATA

In order to compare with experimental results we use the same parameters as used in the deep-inelastic case in Ref. 4. The numerical value of quark masses^{5,8,13} is

$$M_u = M_d = 0.3 \text{ GeV}. \quad (14)$$

Since the mass dependence for large q^2 is only logarithmic, the result is insensitive to the variation of quark masses.^{4,8} The strong coupling constant $\alpha_s = 0.32$, and parton momentum distribution functions $g(x), u(x), d(x)$ are also those used in Ref. 4.

In Fig. 3 the differential cross section $(d^2\sigma/dm dy)|_{y=0}$ ($m = \sqrt{q^2}$) versus m is shown. Our results fit the two sets of data by Hom *et al.*¹⁰ and one by Kluberg *et al.*¹¹ very well. We also plotted a curve for $s = 2000 \text{ GeV}^2$ hoping further higher-energy data may be compared with this.

After y integration we obtain $d\sigma/dm$ and compare with the data by Kluberg *et al.*¹¹ in Fig. 4. Our results are in good agreement with data both of 300-GeV and 400-GeV proton-beam experiments. Note also that our computation for $s = 2800 \text{ GeV}^2$ lies below the ISR bound.¹²

Color has become so central to our thinking

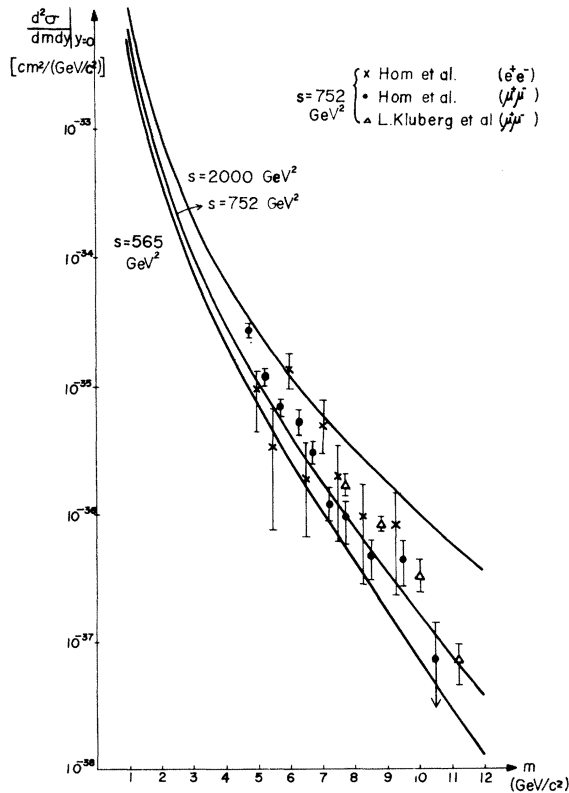


FIG. 3. Plot of $d^2\sigma/dm dy|_{y=0}$ versus m . The data points are from Refs. 10 and 11, all with $s = 752 \text{ GeV}^2$.

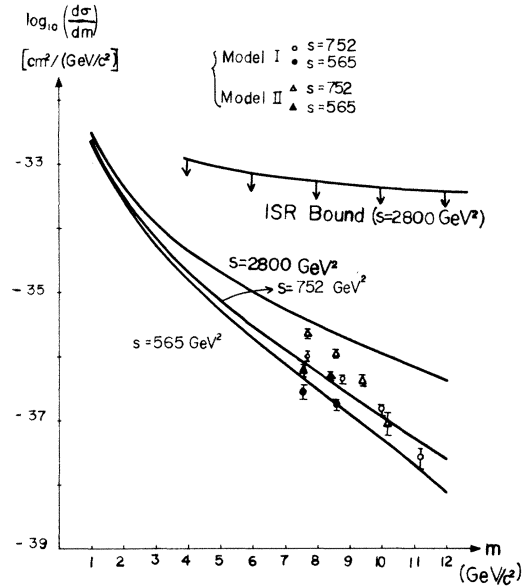


FIG. 4. The cross section $d\sigma/dm$ versus m , with experimental data from Ref. 11. Our results are far below the ISR bound for $s = 2800 \text{ GeV}^2$. L. Kluberg *et al.*, analyzed their data by two models I and II.

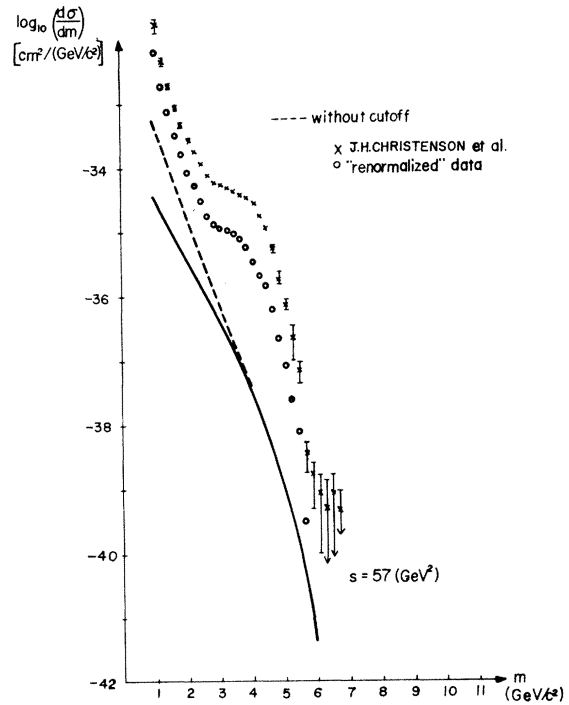


FIG. 5. Cross section $d\sigma/dm$ for $s = 57 \text{ GeV}^2$. Data points are from Ref. 9, dashed line represents the model calculation, and solid line shows the result with longitudinal momentum cutoff ($Q_L > 12 \text{ GeV}/c$), which is the experimental constraint. Renormalized data by G. Farrar (Ref. 19) are also given.

about quark binding and confinement¹⁴ that many theorists would like to have it. It is somewhat reassuring that our model with color agrees quite well with the experimental data.

Our theory disagrees with data from the lower-energy experiment ($s = 57 \text{ GeV}^2$) by Christensen *et al.*,⁹ as shown in Fig. 5. In particular, the disagreement is worse in the $m = 3\text{--}5 \text{ GeV}/c^2$ region, where one is running up against the kinematic limit. This low-energy disagreement is already well known for the Drell-Yan-type theories. Specifically, the work by Einhorn and Savit¹⁵ gives the rigorous bounds on massive-lepton-pair production of QPM's. This bound is consistent with our picture as well as other QPM's. See Ref. 15 for the possible interpretations of the disagreement. One of the reasons for the disagreement considered in Ref. 15 is that the energy ($s = 60 \text{ GeV}^2$) is not high enough to reach the scaling region. This view is quite consistent with what we see in Fig. 2. One may consider other mechanisms which are dominating in this low-energy region.¹⁶⁻¹⁸

IV. SUMMARY

In order to study the lepton-pair production in proton-proton scattering we used a modified QPM which was introduced in Ref. 4. In this model the virtual photon is produced via Compton-like scattering of gluon and quark instead of quark-anti-quark annihilation. Using the same parameters (α_s, M_w, M_d) and the parton distribution functions as in the deep-inelastic reactions, we obtained very good agreement with experimental data for high-energy ($s = 565, 752 \text{ GeV}^2$) cases with color included. For low energy ($s = 57 \text{ GeV}^2$) there is a disagreement which shows up in other Drell-Yan-type models also.

ACKNOWLEDGMENT

One of us (K.S.) would like to thank the members of Cornell Laboratory of Nuclear Studies where this work was started, in particular Professor T.-M. Yan for helpful discussions.

¹S. D. Drell and T.-M. Yan, *Phys. Rev. Lett.* **25**, 316 (1970); *Ann. Phys. (N.Y.)* **66**, 578 (1971).

²See, for example, S. M. Berman *et al.*, *Phys. Rev. D* **4**, 3388 (1971); P. V. Landshoff and J. C. Polkinghorne, *Nucl. Phys.* **B33**, 221 (1971); G. R. Farrar *ibid.* **B77**, 429 (1974); R. McElhaney and S. F. Tuan, *Phys. Rev. D* **8**, 2267 (1973); H. Paar and E. Paschos, *ibid.* **10**, 1502 (1974); S. F. Tuan *et al.*, *ibid.* **10**, 2124 (1974); **11**, 214 (1975).

³R. P. Feynman, *Photon-Hadron Interactions* (Benjamin, Reading, Mass., 1972).

⁴K. S. Soh, *Phys. Rev. D* **13**, 2954 (1976).

⁵See also M. B. Einhorn and S. D. Ellis, *Phys. Rev. Lett.* **34**, 1190 (1975); *Phys. Rev. D* **12**, 2007 (1975), for a similar choice of gluon distribution functions.

⁶V. Barger and R. J. N. Phillips, *Nucl. Phys.* **B73**, 269 (1974).

⁷See, for example, J. Kuti and V. F. Weisskopf, *Phys. Rev. D* **4**, 3418 (1971); R. Blankenbecler *et al.*, SLAC Report No. SLAC-PUB-1531, 1975 (unpublished).

⁸T. Appelquist and H. D. Politzer, *Phys. Rev. Lett.* **34**, 43 (1975); E. Eichten *et al.*, *ibid.* **34**, 369 (1975).

⁹J. H. Christensen *et al.*, *Phys. Rev. Lett.* **25**, 1523 (1970); *Phys. Rev. D* **8**, 2016 (1973).

¹⁰D. C. Hom *et al.*, *Phys. Rev. Lett.* **36**, 1236 (1976); **37**, 1374 (1976).

¹¹L. Kluberg *et al.*, *Phys. Rev. Lett.* **37**, 1451 (1976).

¹²F. W. Busser *et al.*, *Phys. Lett.* **48B**, 377 (1974).

¹³M. K. Gaillard, B. W. Lee, and J. L. Rosner, *Rev. Mod. Phys.* **47**, 277 (1975).

¹⁴M. Y. Han and Y. Nambu, *Phys. Rev.* **139**, B1006 (1965).

¹⁵Martin B. Einhorn and Robert Savit, *Phys. Rev. D* **10**, 2785 (1974).

¹⁶Guido Altarelli, R. A. Brandt, and G. Preparata, *Phys. Rev. Lett.* **26**, 42 (1971).

¹⁷S. Pokorski and L. Stodolsky, *Phys. Lett.* **60B**, 84 (1975); L. Montvay, *ibid.* **53B**, 377 (1974).

¹⁸J. J. Sakurai and H. B. Thacker, *Nucl. Phys.* **B76**, 445 (1974); F. M. Renard, *Nuovo Cimento* **29A**, 64 (1975).

¹⁹G. R. Garrar, in *Phenomenology of Hadronic Structure*, proceedings of the X Rencontre de Moriond, 1975, edited by J. Trân Thanh Vân (CNRS, Paris, 1975).

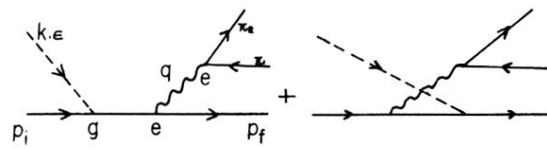


FIG. 1. Feynman diagram of Compton-like scattering. The dashed line represents the gluon; the wavy line represents the photon.

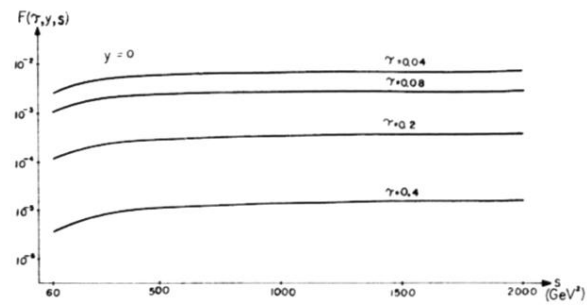


FIG. 2. Scaling behavior of $F(\tau, y, s)$. We plot F versus s for given τ and $y=0$. We see that for about $s < 300 \text{ GeV}^2$ the scaling is not well established in our model.

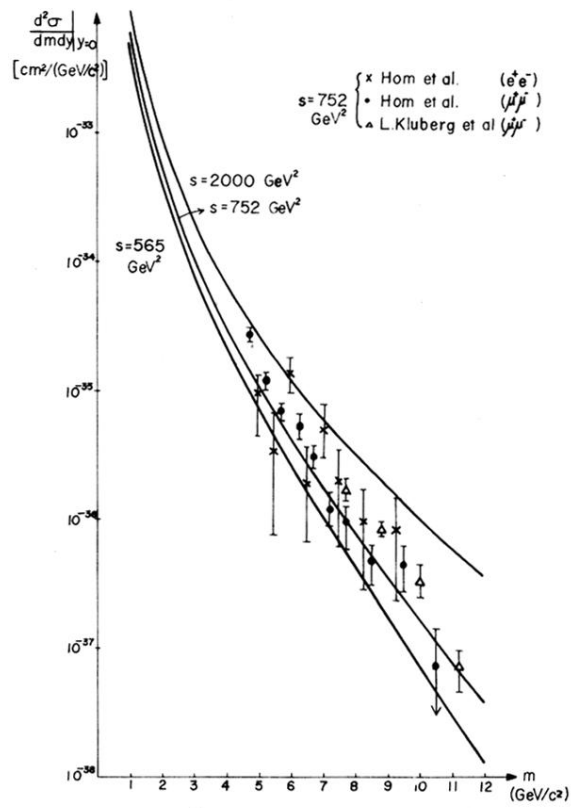


FIG. 3. Plot of $d^2\sigma/dm dy|_{y=0}$ versus m . The data points are from Refs. 10 and 11, all with $s = 752 \text{ GeV}^2$.

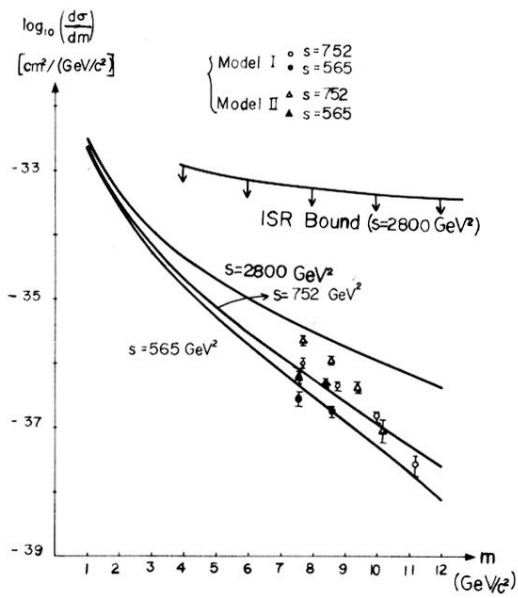


FIG. 4. The cross section $d\sigma/dm$ versus m , with experimental data from Ref. 11. Our results are far below the ISR bound for $s = 2800 \text{ GeV}^2$. L. Kluberg *et al.*, analyzed their data by two models I and II.

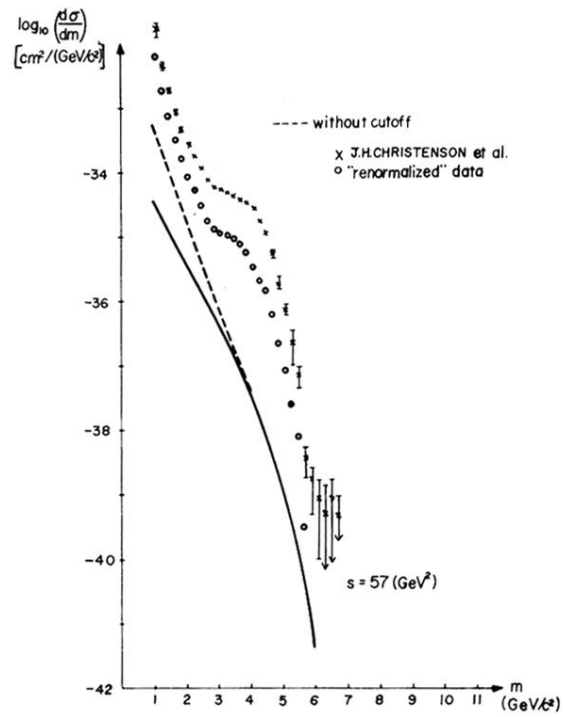


FIG. 5. Cross section $d\sigma/dm$ for $s = 57 \text{ GeV}^2$. Data points are from Ref. 9, dashed line represents the model calculation, and solid line shows the result with longitudinal momentum cutoff ($Q_L > 12 \text{ GeV}/c$), which is the experimental constraint. Renormalized data by G. Farrar (Ref. 19) are also given.